# A Natural Variable Fully Implicit Compositional Reservoir Simulation

**Conference Paper** · November 2017

DOI: 10.20906/CPS/CILAMCE2017-0447



**3 authors**, including:

Bruno Ramon Batista Fernandes
University of Texas at Austin
**30** PUBLICATIONS **76** CITATIONS


# A NATURAL VARIABLE FULLY IMPLICIT COMPOSITIONAL RESERVOIR SIMULATION

**Bruno Ramon Batista Fernandes**

**Kamy Sepehrnoori**

brbfernandes@utexas.edu

kamys@mail.utexas.edu

Center for Petroleum and Geosystems Engineering, The University of Texas at Austin

200 E. Dean Keeton St., Stop C0300, Austin 78712, Texas, USA

**Francisco Marcondes**

marcondes@ufc.br

Department of Metallurgical Engineering and Material Science, Federal University of Ceará, Campus do Pici, Bloco 729, 60.455-760, Ceará, Fortaleza, Brazil

**Abstract.** *The fluid flow in porous media, such as oil reservoirs, is described by complex systems of partial differential equations. Several algorithms to solve these equations have been and continue to be proposed in the literature, each having different impact on convergence rate and computational cost for different scenarios. Numerical formulations differ in their nature due to the level of implicitness degree selected, primary variables and primary equations, and solution algorithm. Fully Implicit algorithms are remarkably important due to their stability, which allows the selection of large time-steps, even for complex reservoirs. In this work, a natural variable formulation, in terms of pressure, phase mole fractions, and saturations is presented for the compositional reservoir simulation based on equation of state using Cartesian grids. In this algorithm, the flow equations are decoupled from the constraint equations (equilibrium relationships) through a Gaussian elimination, significantly reducing the number of variables to be solved in the linear system arising from the discretization of the partial differential equations. The model implemented considers an arbitrary number of components; up to four-phase flow; no mass transfer between the hydrocarbon phases and the aqueous phase; permeability heterogeneity and anisotropy; advection and dispersion. The natural variable formulation is validated with an IMPEC formulation. The results are compared in terms of production data, saturation fronts, and computational cost. It is observed that this new formulation is extremely robust, has low computational cost and requires a low number of iterations per time-step.*

***Keywords:*** *Natural Variable; Fully Implicit Approach; Compositional Reservoir Simulation*



Proceedings of the XXXVIII Iberian Latin-American Congress on Computational Methods in Engineering P.O. Faria, R.H. Lopez, L.F.F. Miguel, W.J.S. Gomes, M. Noronha (Editores), ABMEC, Florianópolis, SC, Brazil, November 5-8, 2017.

# 1 INTRODUCTION

Numerical tools for simulating oil and gas flow in the subsurface and its production are known as reservoir simulators. Most numerical simulators developed assume the oil and gas to be characterized by a single and distinct component. Such model is known as the black-oil model and it obviously fail to describe phenomena such partial vaporization and condensation, gas retrograde condensation, among other processes. In order to model such processes, more components and an equation of state (EoS) that can describe properly the phase behavior are needed. Models that consider such features are called EoS based compositional reservoir models. Due to the coupling of the phase behavior and the material balance equations, several different algorithms can be developed and used to solve the fluid flow with this model. In this paper, special attention is given to the fully implicit algorithms for the compositional reservoir simulation due to its unconditional stability, which allows the algorithm to use larger time-steps for real field reservoirs when compared to other classes of algorithms.

The use of fugacities and an EoS was introduced into the reservoir simulation community by Fussell and Fussel (1979) through an IMPEC formulation (Implicit pressure, explicit compositions). It was readily followed by Coats (1980) who proposed the Natural Variable formulation. A very successfully fully implicit approach that is still being investigated and implemented. Other authors have implemented various fully implicit formulations in the literature (Chien et al., 1985; Collins et al., 1992, Wang et al., 1997; Fernandes et al., 2016; just to name few). Santos et al. (2013) tested several fully implicit, IMPSAT, and IMPEC approaches and notice that the natural variables formulation was, in general, more successfully than the other approaches tested. Several other IMPEC approaches for compositional simulation were also considered through the years (Nghiem et al., 1981; Young and Stepheson, 1983; Acs et al., 1985; to mention few).

The Coats formulation, or Natural Variables formulation, considers $n_c+1$ components, where $n_c$ represents the number of hydrocarbon components and the extra component is the water, which result in $n_c+1$ components. Therefore, $n_c+1$ material balance equations are required. The primary variables considered by this approach are the pressure, phase compositions, and saturations. The fugacity equalities are used as constraint equations.

In this work, the natural variables formulation is implemented and tested. It is implemented into the University of Texas Compositional Reservoir Simulator (UTCOMPRS). UTCOMPRS is a powerful tool initially developed by Chang (1990), Chang et al. (1990), Perschke (1988), Perschke et al. (1989a), and Perschke et al. (1989b) that considers up to four phase flow (water, oil, gas, and a second oleic phase) with rigorous flash and phase stability calculations. UTCOMPRS was originally implemented with the Acs et al. (1985) IMPEC approach for Cartesian grids and has been the subject to several improvements and the addition of new capabilities.

# 2 GOVERNING EQUATIONS

This work considers the isothermal multiphase flow in the porous media. The velocities are modelled according to the multiphase Darcy's law. Mass transfer between the aqueous



Proceedings of the XXXVIII Iberian Latin-American Congress on Computational Methods in Engineering P.O. Faria, R.H. Lopez, L.F.F. Miguel, W.J.S. Gomes, M. Noronha (Editores), ABMEC, Florianópolis, SC, Brazil, November 5-8, 2017.

phase and hydrocarbon phases is neglected. Flow of up to four phases is considered, where the phase equilibria is applied only to the hydrocarbon phases. Advection and dispersion are both considered. The model is also prepared to handle reservoir heterogeneity and inactive cells.

The material balance for each hydrocarbon component can be written as

$$\frac{1}{V_b}\frac{\partial N_k}{\partial t} = \sum_{j=2}^{n_p}\left[\vec{\nabla}\cdot\left(x_{kj}\xi_j\frac{k_{rj}}{\mu_j}\bar{\bar{K}}\cdot\left(\vec{\nabla}P_j-\rho_j g\vec{\nabla}D\right)\right)+\vec{\nabla}\cdot\left(\phi S_j\xi_j\bar{\bar{\Lambda}}_{ij}\cdot\vec{\nabla}x_{ij}\right)\right]-\frac{\dot{q}_k}{V_b},\quad k=1,...,n_c, \quad (1)$$

and for water

$$\frac{1}{V_b}\frac{\partial N_w}{\partial t} = \vec{\nabla}\cdot\left(\xi_w\frac{k_{rw}}{\mu_w}\bar{\bar{K}}\cdot\left(\vec{\nabla}P_w-\rho_w g\vec{\nabla}D\right)\right)-\frac{\dot{q}_w}{V_b}, \quad (2)$$

where $P_j$ is the pressure of phase $j$, $k_{rj}$, $\xi_j$, and $\mu_j$ are the relative permeability, the molar density, and viscosity of phase $j$, respectively. $\bar{\bar{K}}$ is the absolute permeability tensor, $V_b$ is the bulk volume, $x_{kj}$ is the molar fraction of component $k$ in phase $j$, $\dot{q}_k$ is the source/sink term of component $k$ due to the producing/injecting well, $\rho_j$ is the mass density of phase $j$, $g$ is the gravity acceleration, $D$ is the depth, which is positive in the downward direction, $S_j$ is the saturation of phase $j$, $\phi$ is the porosity, and $\bar{\bar{\Lambda}}_{ij}$ is the dispersion tensor of component $i$ in phase $j$. Herein, the subscript $w$ stands for water component or phase, and will be used interchangeably along with the subscripts *1*, for aqueous phase, and $n_c$*+1* for the water component. Similarly, subscripts *2* and *o* stands for oil phase, *3* and *g* for gas phase, and *4* and *l* stand for a second oleic phase. In UTCOMPRS, the phase pressures are computed with respect to the oleic pressure according to the capillary relationship

$$P_j = P + P_{cjo} \qquad j=1,...,n_p, \quad (3)$$

where $P$ is the oleic pressure and $P_{cjo}$ is the capillary pressure of phase $j$ with respect to the reference phase (oil).

The dispersion considers both molecular and mechanical dispersion and the Young (1990) model, Chang (1990).

The Peng-Robinson equation of state (EOS) (Peng and Robinson, 1976) is used to compute density and fugacities. Phase appearance and disappearance is treated using a stability test calculation. Two phase stability test algorithms are implemented in the UTCOMPRS simulator: the stationary point location method (Michelsen, 1982) and the Gibbs free energy minimization algorithm that is similar to the Trangenstein (1987) method and was modified by Perschke (1988) to deal with the equilibrium of three hydrocarbon phases. Phase disappearance is also considered when the saturation of a phase goes below zero.

The constraint equations are the fugacity equalities given as

$$\ln f_{kj} - \ln f_{kr} = 0 \qquad j=3,...,n_p, \quad k=1,...,n_c, \quad (4)$$

where $f_{ij}$ is the fugacity of component $i$ in phase $j$, and $r$ is a reference phase.

# 3 APPROXIMATE EQUATIONS

The finite volume method is used to obtain the approximate equations for the material balances. Integrating Eqs. (1) in time and into the Cartesian control volume presented in Fig. 1, evaluating all variables implicitly, and using the residual form, one obtains

$$\begin{aligned} R_{k,p}^{N} = -\left(N_{k,p}^{n+1} - N_{k,p}^{n}\right) + \Delta t \sum_{j=2}^{n_p} \left[ F_{kj,e}^{n+1} - F_{kj,w}^{n+1} + F_{kj,n}^{n+1} - F_{kj,s}^{n+1} + F_{kj,f}^{n+1} - F_{kj,b}^{n+1} \right] \\ + \Delta t \sum_{j=2}^{n_p} \left[ J_{kj,e}^{n+1} - J_{kj,w}^{n+1} + J_{kj,n}^{n+1} - J_{kj,s}^{n+1} + J_{kj,f}^{n+1} - J_{kj,b}^{n+1} \right] \\ - \Delta t \dot{q}_{k,p}^{n+1}, \quad k = 1, ..., n_c, \end{aligned} \tag{5}$$

where $F_{kj,e}$ is the advective mole flux of component $k$ in phase $j$ through the interface $e$ and $J_{kj,e}$ is the dispersive mole flux of component $k$ in phase $j$ through the interface $e$. The advective mole fluxes are written as

$$F_{kj,r}^{n+1} = \left(x_{kj}^{n+1} \xi_j^{n+1} \lambda_j^{n+1}\right)_r T_r \left[ P_R^{n+1} - P_p^{n+1} + P_{cjr,R}^{n+1} - P_{cjr,p}^{n+1} - \rho_{j,r}^{n+1} g \left(D_R - D_p\right) \right], \tag{6}$$

where $T_r$ is the transmissivity at the interface $r$, and $r$ is any interface (*e*, *w*, *n*, *s*, *f*, or *b*) and $R$ is the gridblock that shares interface $r$ with the gridblock $P$.

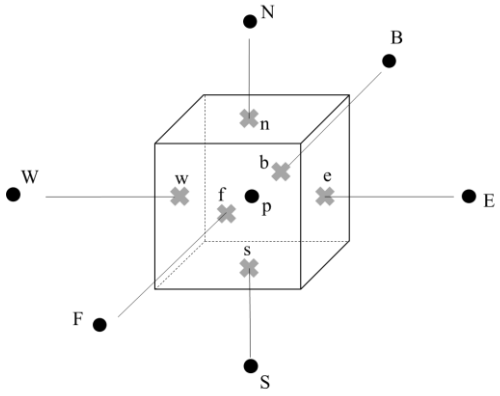


Figure 1. Illustration of a Cartesian Control-Volume with indexations according to Maliska (2004).

The dispersive mole fluxes in the x-direction are computed as

$$\begin{aligned} J_{kj,e}^{n+1} = \Delta Y_p \Delta Z_p \Bigg[ & 2\left(\phi^{n+1} \xi_j^{n+1} S_j^{n+1} \Lambda_{xx,ij}^{n+1}\right)_e \frac{x_{ij,E}^{n+1} - x_{ij,p}^{n+1}}{\Delta X_p + \Delta X_E} \\ & + \left(\phi^{n+1} \xi_j^{n+1} S_j^{n+1} \Lambda_{xy,ij}^{n+1}\right)_e \frac{x_{ij,Ne}^{n+1} - x_{ij,Se}^{n+1}}{\Delta Y_p + 0.5\left(\Delta Y_N + \Delta Y_S\right)} \\ & + \left(\phi^{n+1} \xi_j^{n+1} S_j^{n+1} \Lambda_{xz,ij}^{n+1}\right)_e \frac{x_{ij,Fe}^{n+1} - x_{ij,Be}^{n+1}}{\Delta Z_p + 0.5\left(\Delta Z_F + \Delta Z_B\right)} \Bigg] \end{aligned}, \tag{7}$$

$$J_{kj,w}^{n+1} = \Delta Y_p \Delta Z_p \left[ 2\left(\phi^{n+1}\xi_j^{n+1}S_j^{n+1}\Lambda_{xx,ij}^{n+1}\right)_w \frac{x_{ij,W}^{n+1} - x_{ij,p}^{n+1}}{\Delta X_p + \Delta X_W} \right.$$
$$+\left(\phi^{n+1}\xi_j^{n+1}S_j^{n+1}\Lambda_{xy,ij}^{n+1}\right)_w \frac{x_{ij,Nw}^{n+1} - x_{ij,Sw}^{n+1}}{\Delta Y_p + 0.5\left(\Delta Y_N + \Delta Y_S\right)} \quad . \tag{8}$$
$$\left. +\left(\phi^{n+1}\xi_j^{n+1}S_j^{n+1}\Lambda_{xz,ij}^{n+1}\right)_w \frac{x_{ij,Fw}^{n+1} - x_{ij,Bw}^{n+1}}{\Delta Z_p + 0.5\left(\Delta Z_F + \Delta Z_B\right)} \right]$$

The dispersive mole fluxes for the other interfaces are obtained similarly.

The constraint equations for each grid block are given by Eq. (4). In the residual form, this restriction is given by

$$R_{kj}^F = \ln f_{P,kj} - \ln f_{P,kr} \qquad j = 3,...,n_p, \quad k = 1,...,n_c, \tag{9}$$

# 4 NATURAL VARIABLES FORMULATION

In the natural variables formulation, the unknowns are the reference pressure, $n_p$*-1* saturations, and *(*$n_p$*-1)(*$n_c$*-1)* compositions. All other variables are determined through material balance constraints or other relationships. The total number of unknowns per gridblock is then $n_p$*+(*$n_p$*-1)(*$n_c$*-1)*. However, through the Gibbs phase rule and knowing that temperature does not change for the isothermal considered in this work, one can observe that only $n_c$*+1* equations will determine the whole system, thanks to the thermodynamics relationships (the fugacity equality). These $n_c$*+1* unknowns are called primary variables, and the rest of the unknowns are the secondary variables. In this formulation, pressure and saturations are always considered primary variables, while $n_c$*+1-*$n_p$ are phase compositions. Since Equations (5) and (9) are strongly non-linear, the Newton-Raphson method is used in order to obtain the solution. Through Newton's method one obtains

$$\bar{\bar{J}}_k^{n+1} \Delta \vec{x}_k^{n+1} = -\vec{r}_k^{n+1}, \tag{10}$$

where $\Delta \vec{x}_k^{n+1}$ are the changes in the primary variables at iteration *k*, $\vec{r}_k^{n+1}$ are the residues of the volume balance and material balances at iteration *k*, and $\bar{\bar{J}}_k^{n+1}$ is the Jacobian matrix at iteration *k*. For better illustration, Eq. (10) is written for a 1D grid using a blocked Jacobian, blocked vector unknowns, and blocked vector residues vector below.

$$\begin{bmatrix}
A_{1,P} & B_{1,P} & A_{1,E} & B_{1,E} & & & & & & & & \\
C_1 & D_1 & 0 & 0 & & & & & & & & \\
A_{2,W} & B_{2,W} & A_{2,P} & B_{2,P} & A_{2,E} & B_{2,E} & & & & & & \\
0 & 0 & C_2 & D_2 & 0 & 0 & & & & & & \\
 & & \ddots & & \ddots & & \ddots & & & & & \\
 & & & & A_{n_B-1,W} & B_{n_B-1,W} & A_{n_B-1,P} & B_{n_B-1,P} & A_{n_B-1,E} & B_{n_B-1,E} & & \\
 & & & & 0 & 0 & C_{n_B-1} & D_{n_B-1} & 0 & 0 & & \\
 & & & & & & A_{n_B,W} & B_{n_B,W} & A_{n_B,P} & B_{n_B,P} & & \\
 & & & & & & 0 & 0 & C_{n_B} & D_{n_B} & &
\end{bmatrix}
\begin{bmatrix} \Delta X_{P1} \\ \Delta X_{S1} \\ \Delta X_{P2} \\ \Delta X_{S2} \\ \vdots \\ \Delta X_{Pn_B-1} \\ \Delta X_{Sn_B-1} \\ \Delta X_{Pn_B} \\ \Delta X_{Sn_B} \end{bmatrix}
= -
\begin{bmatrix} R_{P1} \\ R_{S1} \\ R_{P2} \\ R_{S2} \\ \vdots \\ R_{Pn_B-1} \\ R_{Sn_B-1} \\ R_{Pn_B} \\ R_{Sn_B} \end{bmatrix}, \tag{11}$$

where $A_{i,j}$ is the matrix with the derivatives of the material balance residues of gridblock $i$ with respect to the primary variables of gridblock $P$, $B_{i,j}$ is the matrix with the derivatives of the material balance residues of gridblock $i$ with respect to the secondary variables of gridblock $P$, $C_i$ is the matrix with the derivatives of the fugacity residues of gridblock $i$ with respect to the primary variables of gridblock $i$, and $D_i$ is the matrix with the derivatives of the fugacity residues of gridblock $i$ with respect to the secondary variables of gridblock $i$.

Solving the whole system is too expensive. However, one may notice that C and D are present only on main diagonals, once the fugacities are functions only of the gridblock unknowns. Due to this fact, a Gaussian elimination can be used to make all B's zero in the matrix of Eq. (11). Once $B$ is eliminated, the secondary variables can be decoupled from the primary variables. To do so, the row that corresponds to the secondary variables is multiplied by the inverse of $D$, resulting in

$$\begin{bmatrix} A_{1,P} & B_{1,P} & A_{1,E} & B_{1,E} & & & & & & & & \\ D_1^{-1}C_1 & I & 0 & 0 & & & & & & & & \\ A_{2,W} & B_{2,W} & A_{2,P} & B_{2,P} & A_{2,E} & B_{2,E} & & & & & & \\ 0 & 0 & D_2^{-1}C_2 & I & 0 & 0 & & & & & & \\ & & \ddots & & \ddots & & \ddots & & & & & \\ & & & & A_{n_B-1,W} & B_{n_B-1,W} & A_{n_B-1,P} & B_{n_B-1,P} & A_{n_B-1,E} & B_{n_B-1,E} & & \\ & & & & 0 & 0 & D_{n_B-1}^{-1}C_{n_B-1} & I & 0 & 0 & & \\ & & & & & & A_{n_B,W} & B_{n_B,W} & A_{n_B,P} & B_{n_B,P} & & \\ & & & & & & 0 & 0 & D_{n_B}^{-1}C_{n_B} & I & & \end{bmatrix} \begin{bmatrix} \Delta X_{P1} \\ \Delta X_{S1} \\ \Delta X_{P2} \\ \Delta X_{S2} \\ \vdots \\ \Delta X_{Pn_B-1} \\ \Delta X_{Sn_B-1} \\ \Delta X_{Pn_B} \\ \Delta X_{Sn_B} \end{bmatrix} = - \begin{bmatrix} R_{P1} \\ D_1^{-1}R_{S1} \\ R_{P2} \\ D_2^{-1}R_{S2} \\ \vdots \\ R_{Pn_B-1} \\ D_{n_B-1}^{-1}R_{Sn_B-1} \\ R_{Pn_B} \\ D_{n_B}^{-1}R_{Sn_B} \end{bmatrix}. \tag{12}$$

The row of the secondary variables is then multiplied by B and subtracted from the row of the primary variables

$$\begin{bmatrix} A_{1,P}-B_{1,P}D_1^{-1}C_1 & 0 & A_{1,E} & B_{1,E} & & & & & & & & \\ D_1^{-1}C_1 & I & 0 & 0 & & & & & & & & \\ A_{2,W} & B_{2,W} & A_{2,P}-B_{2,P}D_2^{-1}C & 0 & A_{2,E} & B_{2,E} & & & & & & \\ 0 & 0 & D_2^{-1}C_2 & I & 0 & 0 & & & & & & \\ & & \ddots & & \ddots & & \ddots & & & & & \\ & & & & A_{n_B-1,W} & B_{n_B-1,W} & A_{n_B-1,P}-B_{n_B-1,P}D_{n_B-1}^{-1}C_{n_B-1} & 0 & A_{n_B-1,E} & B_{n_B-1,E} & & \\ & & & & 0 & 0 & D_{n_B-1}^{-1}C_{n_B-1} & I & 0 & 0 & & \\ & & & & & & A_{n_B,W} & B_{n_B,W} & A_{n_B,P}-B_{n_B,P}D_{n_B}^{-1}C_{n_B} & 0 & & \\ & & & & & & 0 & 0 & D_{n_B}^{-1}C_{n_B} & I & & \end{bmatrix} \begin{bmatrix} \Delta X_{P1} \\ \Delta X_{S1} \\ \Delta X_{P2} \\ \Delta X_{S2} \\ \vdots \\ \Delta X_{Pn_B-1} \\ \Delta X_{Sn_B-1} \\ \Delta X_{Pn_B} \\ \Delta X_{Sn_B} \end{bmatrix} = - \begin{bmatrix} R_{P1}-B_{1,P}D_1^{-1}R_{S1} \\ D_1^{-1}R_{S1} \\ R_{P2}-B_{2,P}D_2^{-1}R_{S2} \\ D_2^{-1}R_{S2} \\ \vdots \\ R_{Pn_B-1}-B_{n_B-1,P}D_{n_B-1}^{-1}R_{Sn_B-1} \\ D_{n_B-1}^{-1}R_{Sn_B-1} \\ R_{Pn_B}-B_{n_B,P}D_{n_B}^{-1}R_{Sn_B} \\ D_{n_B}^{-1}R_{Sn_B} \end{bmatrix}. \tag{13}$$

With the $B$ from the main diagonal eliminated, one can proceed the eliminating of the off diagonal $B$.

$$
\begin{bmatrix}
A_{1,P}-B_{1,P}D_1^{-1}C_1 & 0 & A_{1,E}-B_{1,E}D_2^{-1}C_2 & 0 & & & & \\
D_1^{-1}C_1 & I & 0 & 0 & & & & \\
A_{2,W}-B_{2,W}D_1^{-1}C_1 & 0 & A_{2,P}-B_{2,P}D_2^{-1}C_2 & 0 & A_{2,E}-B_{2,E}D_3^{-1}C_3 & 0 & & \\
0 & 0 & D_2^{-1}C_2 & I & 0 & 0 & & \\
 & & \ddots & & \ddots & & \ddots & \\
 & & & & A_{n_B-1,W}-B_{n_B-1,W}D_{n_B-2}^{-1}C_{n_B-2} & 0 & A_{n_B-1,P}-B_{n_B-1,P}D_{n_B-1}^{-1}C_{n_B-1} & 0 \\
 & & & & 0 & 0 & D_{n_B-1}^{-1}C_{n_B-1} & I \\
 & & & & & & A_{n_B,W}-B_{n_B,W}D_{n_B-1}^{-1}C_{n_B-1} & 0 \\
 & & & & & & 0 & 0
\end{bmatrix}
\begin{bmatrix}
\Delta X_{P1} \\ \Delta X_{S1} \\ \Delta X_{P2} \\ \Delta X_{S2} \\ \vdots \\ \Delta X_{Pn_B-1} \\ \Delta X_{Sn_B-1} \\ \Delta X_{Pn_B} \\ \Delta X_{Sn_B}
\end{bmatrix}
$$

$$
=-\begin{bmatrix}
R_{P1}-\sum_{k=1}^{n_{nb}} B_{1,V_k}D_{V_k}^{-1}R_{SV_k} \\
D_1^{-1}R_{S1} \\
R_{P2}-\sum_{k=1}^{n_{nb}} B_{2,V_k}D_{V_k}^{-1}R_{SV_k} \\
D_2^{-1}R_{S2} \\
\vdots \\
R_{Pn_B-1}-\sum_{k=1}^{n_{nb}} B_{n_B-1,V_k}D_{V_k}^{-1}R_{SV_k} \\
D_{n_B-1}^{-1}R_{Sn_B-1} \\
R_{Pn_B}-\sum_{k=1}^{n_{nb}} B_{n_B,V_k}D_{V_k}^{-1}R_{SV_k} \\
D_{n_B}^{-1}R_{Sn_B}
\end{bmatrix}, \tag{14}
$$

where $n_{nb}$ is the number of neighbors from the gridblock, considering itself as a neighbor, and $v_k$ is the index of that neighbor (*P*, *E*, *W*, *N*, *S*, *F*, *B*). After B is eliminated, it can be observed that the secondary variables can be obtained as

$$\Delta X_{SP} = D_P^{-1}R_{SP} - D_P^{-1}C_P\Delta X_{PP}, \tag{15}$$

and the linear system from Eq. (14) can be rewritten as

$$
\begin{bmatrix}
A_{1,P}-B_{1,P}D_1^{-1}C_1 & A_{1,E}-B_{1,E}D_2^{-1}C_2 & & & \\
A_{2,W}-B_{2,W}D_1^{-1}C_1 & A_{2,P}-B_{2,P}D_2^{-1}C_2 & A_{2,E}-B_{2,E}D_3^{-1}C_3 & & \\
 & \ddots & \ddots & \ddots & \\
 & & A_{n_B-1,W}-B_{n_B-1,W}D_{n_B-2}^{-1}C_{n_B-2} & A_{n_B-1,P}-B_{n_B-1,P}D_{n_B-1}^{-1}C_{n_B-1} & A_{n_B-1,E}-B_{n_B-1,E}D_{n_B}^{-1}C_{n_B} \\
 & & & A_{n_B,W}-B_{n_B,W}D_{n_B-1}^{-1}C_{n_B-1} & A_{n_B,P}-B_{n_B,P}D_{n_B}^{-1}C_{n_B}
\end{bmatrix}
\begin{bmatrix}
\Delta X_{P1} \\ \Delta X_{P2} \\ \vdots \\ \Delta X_{Pn_B-1} \\ \Delta X_{Pn_B}
\end{bmatrix}
$$

$$
=-\begin{bmatrix}
R_{P1}-\sum_{k=1}^{n_{nb}} B_{1,V_k}D_{V_k}^{-1}R_{SV_k} \\
R_{P2}-\sum_{k=1}^{n_{nb}} B_{2,V_k}D_{V_k}^{-1}R_{SV_k} \\
\vdots \\
R_{Pn_B-1}-\sum_{k=1}^{n_{nb}} B_{n_B-1,V_k}D_{V_k}^{-1}R_{SV_k} \\
R_{Pn_B}-\sum_{k=1}^{n_{nb}} B_{n_B,V_k}D_{V_k}^{-1}R_{SV_k}
\end{bmatrix}. \tag{16}
$$

Equation (16) is used to update the primary variables, followed by Eq. (15) to update the secondary variables. The procedure presented here can be easily extended to 2D and 3D grids. In fact, it can be extended for any type of grid (structured corner point or unstructured grid).

# 5 RESULTS

In this work, four case studies are investigated. The first case study considers $CO_2$ injection in a heterogeneous reservoir at constant surface rate. The second case is very similar

to the first, but the reservoir has an irregular geometry that is discretized using inactive cells, and is strongly heterogeneous. Also, the $CO_2$ rich fluid is injected at a constant bottom hole pressure. The third case is a gas/solvent injection in a heterogeneous reservoir, which contains a gas cap initially. Finally, the last case study considers the $CO_2$ injection in a heterogeneous reservoir with irregular geometry. This case differs from all the cases, because it considers up to three hydrocarbon phases. The results are compared with the IMPEC formulation originally implemented into UTCOMPRS whenever possible. IMPEC scheme require a limited time-step due to instability issues. Using these approaches alone for heterogeneous reservoirs may be a very challenging problem. Despite of this, we can combine both fully implicit and IMPEC algorithms to further enhance performance while keeping the stability, but this will not be treated in this work. All reservoir geometry and heterogeneity maps are synthetic and were developed to test UTCOMPRS with very challenging cases.

The first case study considers a reservoir with heterogeneity in the permeabilities in the X and Y directions. Also, twenty three wells injecting at constant rate are considered in this case. A 153x77x10 grid is used. The permeability in X is equals to the permeability in Y and the absolute permeability field is presented in Figure 2.

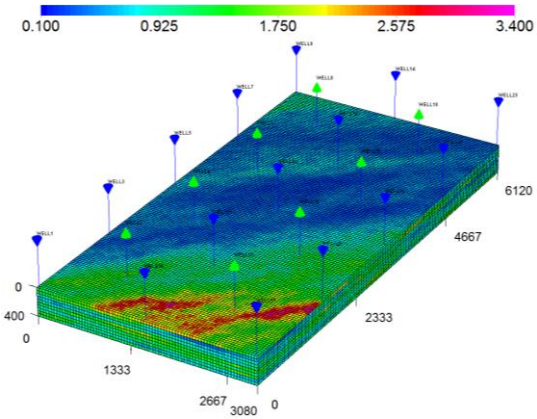


Figure 2. Permeability ($10^{-13}$ $m^2$) in X- and Y- directions distribution for Case 1 (reservoir dimensions in feet).

The reservoir data for this case is presented in Table 1. No physical dispersion is considered in this run and the simulation was performed up to 2190 simulation days (about 0.22 PVI).

A comparison of the oil and gas production rates between the natural variables fully implicit approach implemented in this work and the IMPEC approach is presented in Figure 3, where it can be observed that a good match of the results are obtained. The time-stepping profile is presented in Figure 4, where we can observe that the IMPEC approach was able to reach time-step size up to 1 day. Through our tests, any further increase in this time-step would cause the simulation to eventually fail or cause non-physical oscillation in the solution. On the other hand, the FI approach implemented in this work performed the run mostly at the maximum time-step that was set to 20 days. In fact, it was observed that the FI simulation could be carried out using even large time-steps, but this could lead to unsatisfactory results.

Table 1. Reservoir data for Case 1.

| Property | Value |
|---|---|
| Length, width, and thickness | 1865.37 m, 938.78 m, and 121.92 m |
| Reference Porosity | 0.30 |
| Initial Water Saturation | 0.25 |
| Initial Pressure | 20.68 MPa |
| Permeability in z direction | $9.87\times10^{-15}$ $m^2$ |
| Formation Temperature | 299.82 K |
| Gas Injection Rate | 4.92 $m^3/s$ (internal wells), 2.46 $m^3/s$ (lateral wells), 1.23 $m^3/s$ (corner wells) |
| Producer's Bottom Hole Pressure | 20.68 MPa |
| Reservoir initial composition ($CO_2$, $C_1$, and $nC_{16}$) | 0.01, 0.19, and 0.80 |
| Injection fluid composition ($CO_2$, $C_1$, and $nC_{16}$) | 0.95, 0.05 and 0.00 |

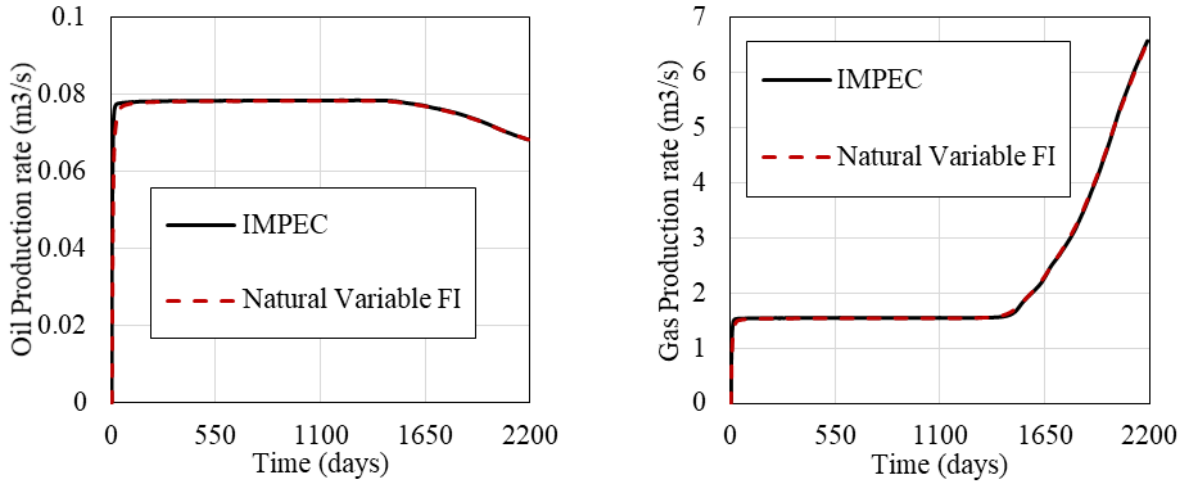


(a) (b)

Figure 3. Production rates for case study 1. a) Oil and b) gas.



Proceedings of the XXXVIII Iberian Latin-American Congress on Computational Methods in Engineering P.O. Faria, R.H. Lopez, L.F.F. Miguel, W.J.S. Gomes, M. Noronha (Editores), ABMEC, Florianópolis, SC, Brazil, November 5-8, 2017.

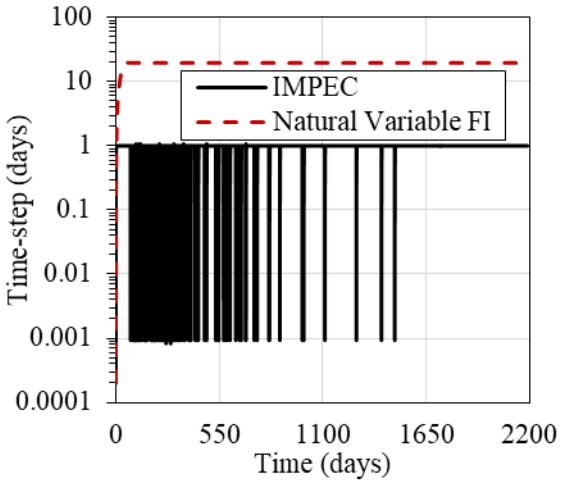


Figure 4. Time-step profile for Case 1.

A very good match of the gas saturation field at 2190 days of simulation time can be observed in Figure 5.

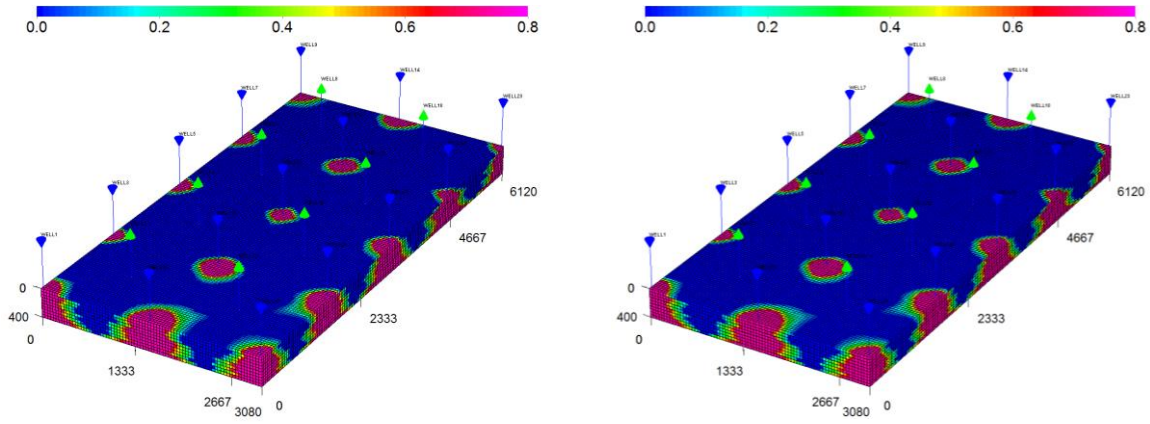


(a) (b)

Figure 5. Gas saturation field for Case 1 at 2190 (grid sizes in feet). a) IMPEC; and b) Natural Variables FI.

The comparison between the CPU times for the IMPEC and natural variables approach is presented in Table 2, where it can be observed that the natural variables is considerably faster than the IMPEC approach.

Table 2. CPU Time for Case 1.

| Formulation | CPU Time (s) | Normalized CPU Time |
|---|---|---|
| IMPEC | 1810.27 | 1.00 |
| Natural Variables FI | 938.59 | 0.52 |

The second case is very similar to the first. However, we replaced the reservoir formation with a more complex one and the injector wells now inject fluid at a constant bottom hole pressure of 21.37 MPa. A 200x400x25 grid is considered, but only 465,816 cells are actually active (about 23% of all gridblocks). Forty-three wells are considered. In the approach implemented here, inactive cells are not allocated and are not included in any calculation, reducing both CPU time and memory required for the runs. The reservoir geometry is presented in Figure 6. The distance from the gridblock center to the reservoir top is colored within the grid. The porosity and permeability maps are presented in Figure 7.

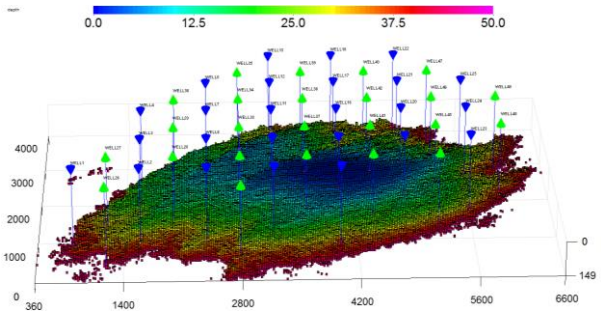


Figure 6. Depth from the gridblock center to the reservoir's top in meters for Case 2 (reservoir dimensions in feet).

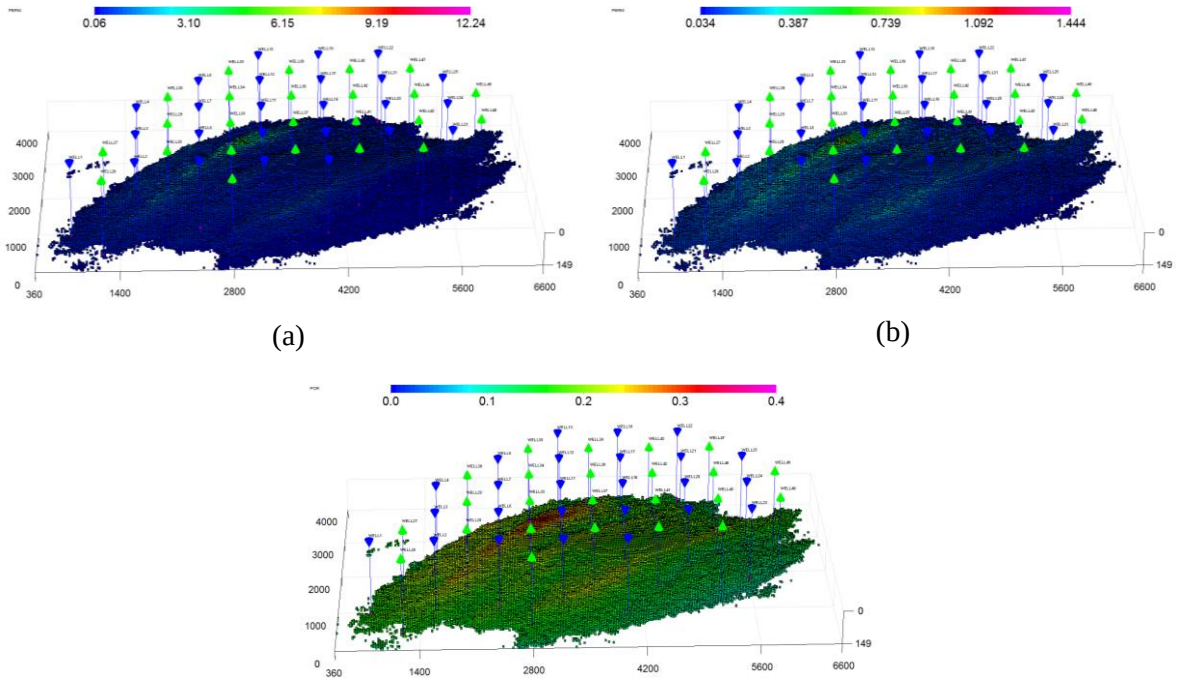


(a) (b)

(c)

Figure 7. Permeability and porosity maps for Case 2 (reservoir dimensions in feet). a) permeability in X and Y directions ($10^{-13}$ $m^2$); b) permeability in Z direction ($10^{-13}$ $m^2$); and c) porosity.

The oil and gas production rates are presented in Figure 8, but they are not compared to the IMPEC approach because it could not finish the simulation, properly.

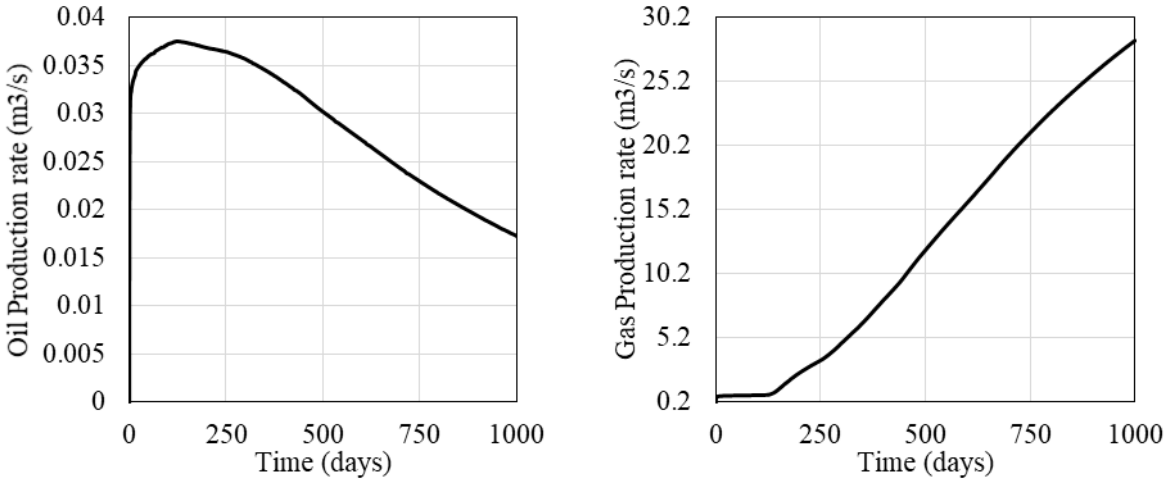


(a) (b)

Figure 8. Production rates for Case 2. a) Oil and b) gas.

The gas saturation field at 1000 days is presented in Figure 9.

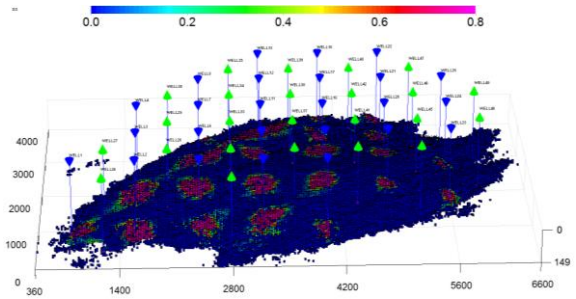


Figure 9. Gas saturation field at 1000 days for Case 2.

The time-step profile is presented in Figure 10.

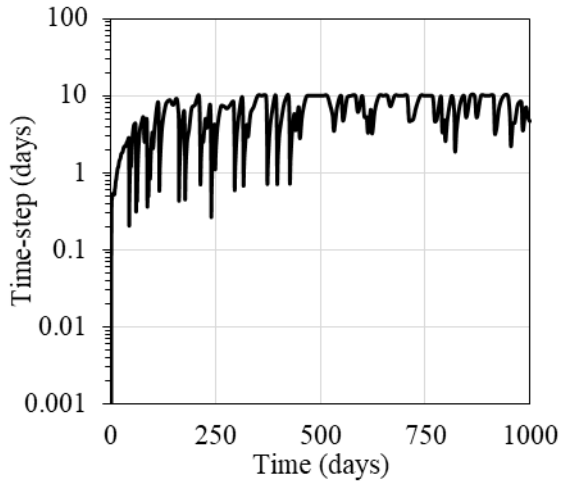


Figure 10. Time-step profile for Case 2.

The CPU time for this run was 10,881.54 seconds.

The third case study considers a gas/solvent injection based on the SPE comparison project presented by Killough and Kossack (1987). The reservoir data is presented in Table 3. Notice that dispersion is considered in this case. Heterogeneity in the permeabilities is considered and presented in Figure 11.

Table 3. Reservoir data for Case 3.

| Property | Value |
|---|---|
| Length, width, and thickness | 170.688 m, 170.688 m, and 30.48 m |
| Reference Porosity | 0.35 |
| Initial Water Saturation | 0.30 |
| Initial Pressure | 10.34 MPa |
| Formation Temperature | 344.26 K |
| Longitudinal Dispersivity | 4.74 m |
| Transverse Dispersivity | 0.47 m |
| Longitudinal parameter for Young's Dispersion | 0.91 |
| Transverse parameter for Young's Dispersion | 0.91 |
| Gas Injection Rate | 0.328 $m^3/s$ |
| Producer's Bottom Hole Pressure | 8.96 MPa |
| Reservoir's initial composition (C1, C3, C6, C10, C15, and C20) | 0.50, 0.03, 0.07, 0.20, 0.15, and 0.05 |
| Injection fluid composition (C1, C3, C6, C10, C15, and C20) | 0.77, 0.20, 0.01, 0.01, 0.005 and 0.005 |



Proceedings of the XXXVIII Iberian Latin-American Congress on Computational Methods in Engineering P.O. Faria, R.H. Lopez, L.F.F. Miguel, W.J.S. Gomes, M. Noronha (Editores), ABMEC, Florianópolis, SC, Brazil, November 5-8, 2017.

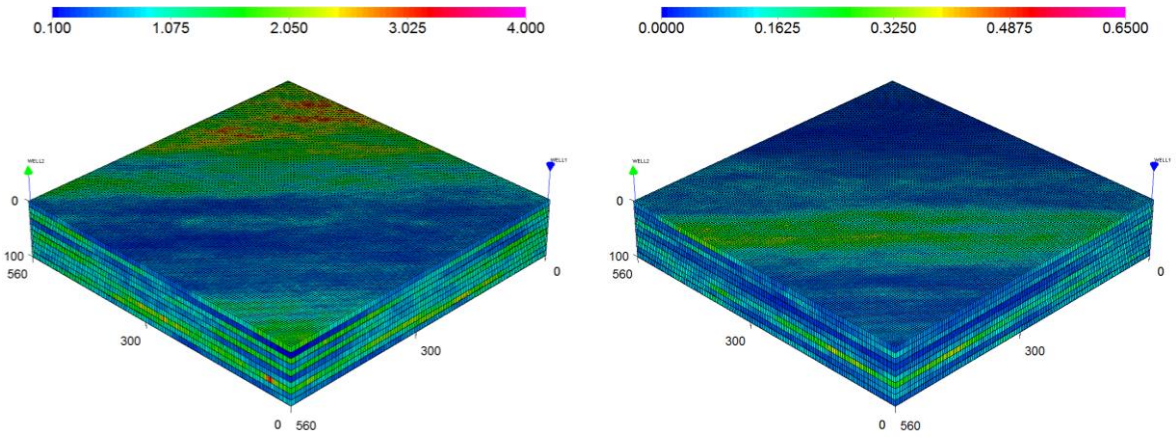


(a) (b)

Figure 11. Permeability distribution ($10^{-13}$ $m^2$) for Case 3. a) X and Y directions and b) Z direction.

A comparison of the production rates obtained with the natural variables against the IMPEC is presented in Figure 12, where a good match can be observed.

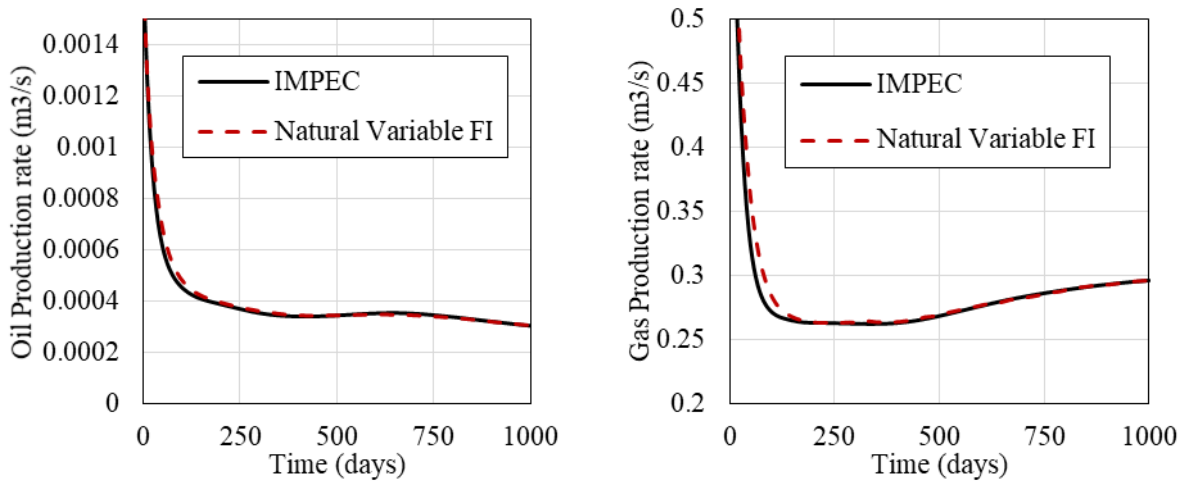


(a) (b)

Figure 12. Production rates for Case 3. a) Oil and b) gas.

A comparison of the gas saturation field at 1000 days is presented in Figure 13, where a good agreement can also be observed between the IMPEC and the Natural Variable approach.

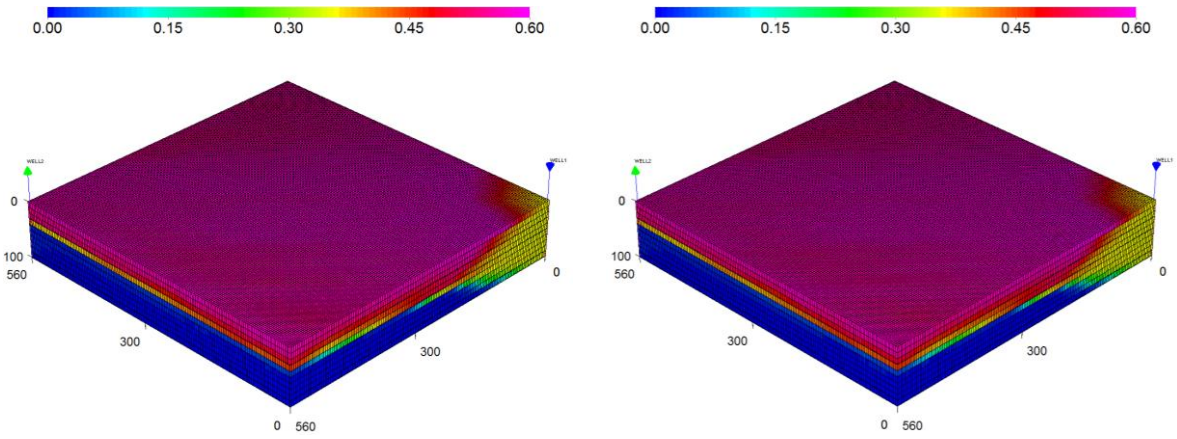


(a) (b)

Figure 13. Gas saturation field for Case 3 at 1000 (grid scale in feet). a) IMPEC and b) Natural Variables FI.

The time-step profile presented in Figure 14 shows a very steady time-step for all formulations. The time-step for the IMPEC formulation is set to not exceed 0.005 days due to the inclusion of oscillations in the production curves and simulation crash. Therefore, one can observe an increase in the time-step of about 4000 times in this case for the FI compared to the IMPEC approach. It was observed that this excessive decrease in time-step size of the IMPEC approach is much related to the effect of dispersion, since the time-step for IMPEC are much larger when dispersion is not considered. As a consequence of such small time-step, the CPU time used for the IMPEC run is considerably bigger than that of the natural variables as presented in Table 4.

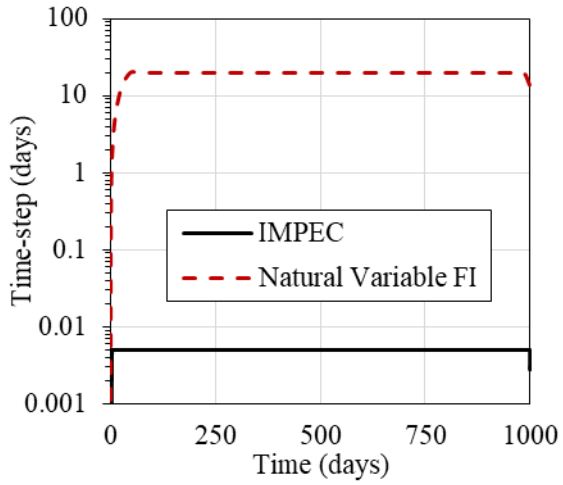


Figure 14. Time-step profile for Case 3.

Table 4. CPU time for Case 3.

| Formulation | CPU Time (s) | Normalized CPU Time |
|---|---|---|
| IMPEC | 703,501.81 | 1.00 |
| Natural Variables FI | 16,656.82 | 0.024 |

The last case study considers a $CO_2$ injection in an irregular and heterogeneous reservoir. The reservoir fluid is the BSB west Texas Oil (Khan et al., 1992) and considers 7 hydrocarbon components. A 200x200x10 grid is used with 99,816 active cells (about 25% of the total cells) and 13 wells. The importance of this case here is to present the capability of our approach to simulate the four phase flow. Herein, a second liquid hydrocarbon phase is formed. The reservoir data is summarized in Table 5. Dispersion, is also considered for this case. The reservoir geometry is presented in Figure 15. The distance from the gridblock center to the reservoir top is colored within the grid. The porosity and permeability maps are presented in Figure 16. The permeability in Z direction is 10 times smaller than those in X and Y directions.

Table 5. Reservoir data for Case 4.

| Property | Value |
|---|---|
| Length, width, and thickness | 1219.2 m, 1219.2 m, and 60.96 m |
| Initial Water Saturation | 0.25 |
| Initial Pressure | 7.58 MPa |
| Formation Temperature | 313.706 K |
| Longitudinal Dispersivity | 4.74 m |
| Transverse Dispersivity | 0.47 m |
| Longitudinal parameter for Young's Dispersion | 9.1 |
| Transverse parameter for Young's Dispersion | 9.1 |
| Injector's Bottom Hole Pressure | 8.62 MPa (all injectors) |
| Producer's Bottom Hole Pressure | 7.58 MPa (all producers) |
| Reservoir's initial composition (CO2, C1, C2-3, C4-6, C7-15, C16-27, and C28+) | 0.0337, 0.0861, 0.1503, 0.1671, 0.3304, 0.1611, and 0.0713 |
| Injection fluid composition (CO2 and C1) | 0.95, 0.05 |

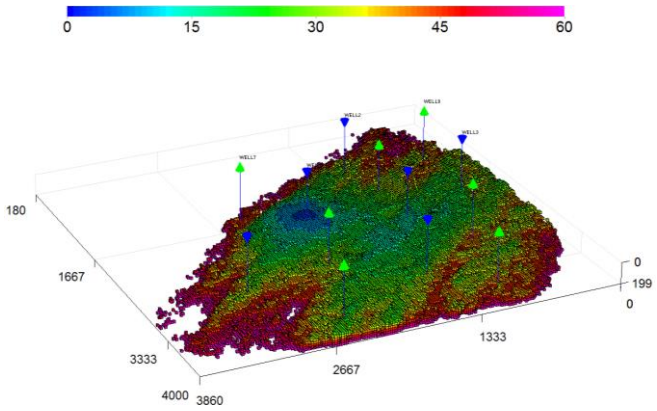


Figure 15. Depth from the gridblock center to the reservoir's top in meters for Case 4 (reservoir dimensions in feet).

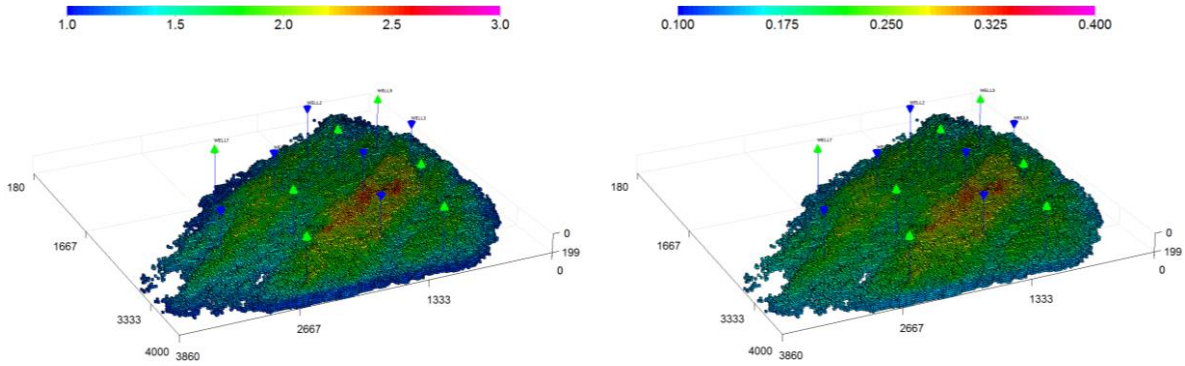


(a) (b)

Figure 16. Permeability and porosity maps for Case 4 (reservoir dimensions in feet). a) permeability in X and Y directions ($10^{-13}$ $m^2$) and b) porosity.

The oil and gas production rates are presented in Figure 17, but once again, they are not compared to the IMPEC approach because it could not finish the simulation properly.

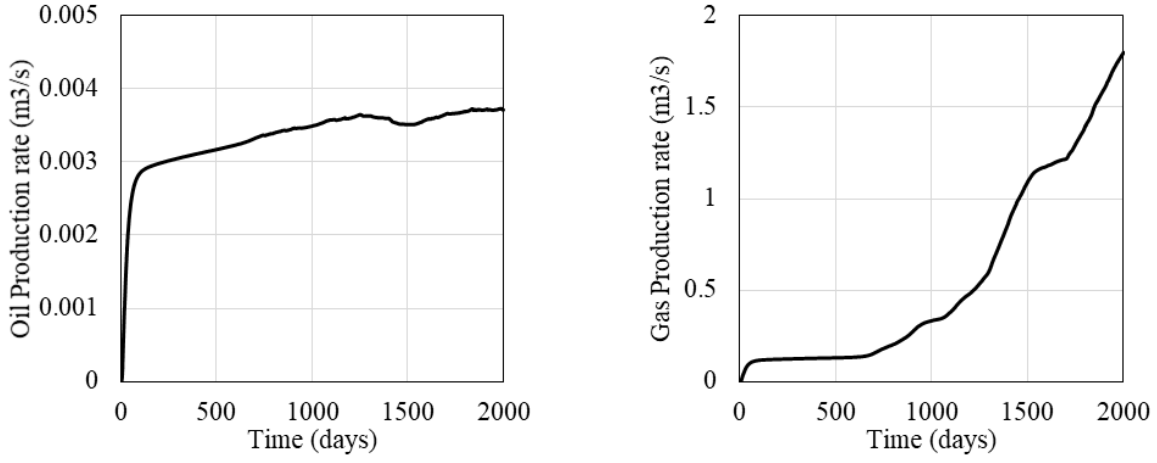


(a) (b)

Figure 17. Production rates for Case 4. a) Oil and b) gas.

The gas saturation, second liquid saturation, and $CO_2$ overall composition at 2000 days of simulation are presented in Figure 18.

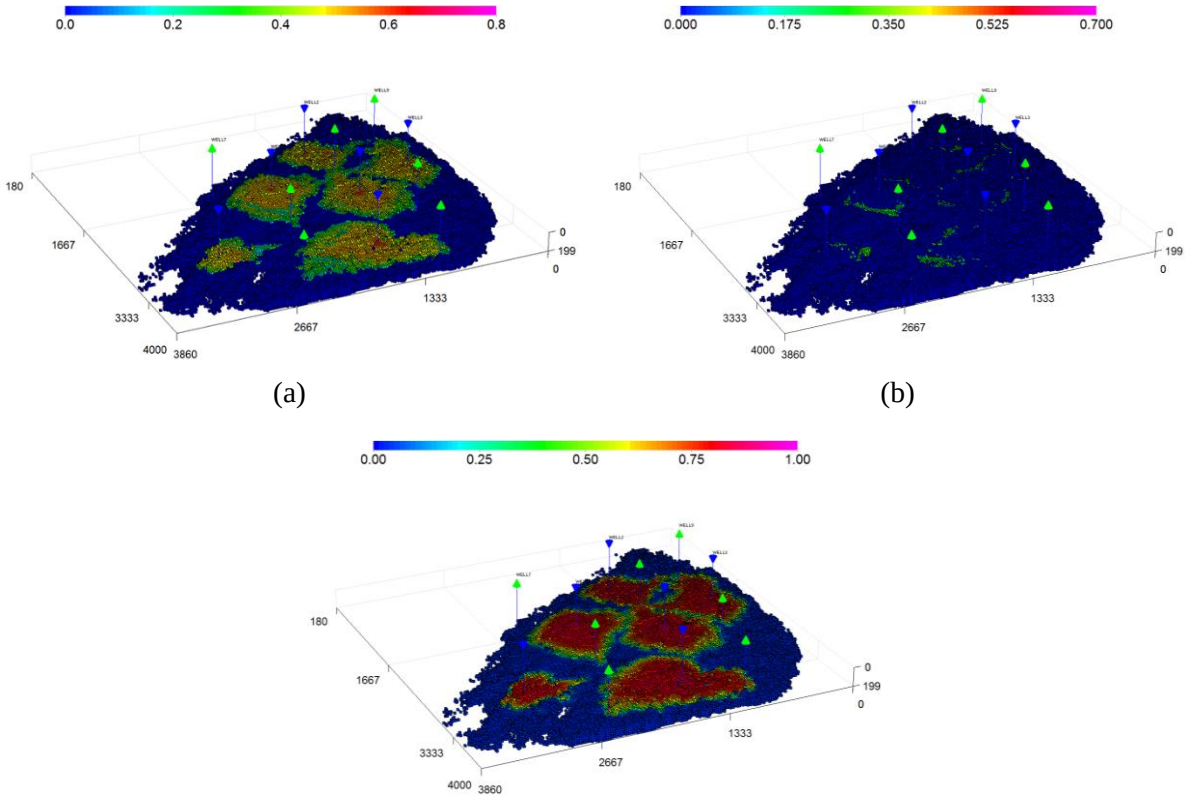


Figure 18. Fields for Case 4 at 2000 (grid scales in feet). a) Gas saturation; b) second liquid saturation; and c) $CO_2$ overall mole fraction.

The time-step profile is presented in Figure 19. The run was completed in 148,358.95 seconds.

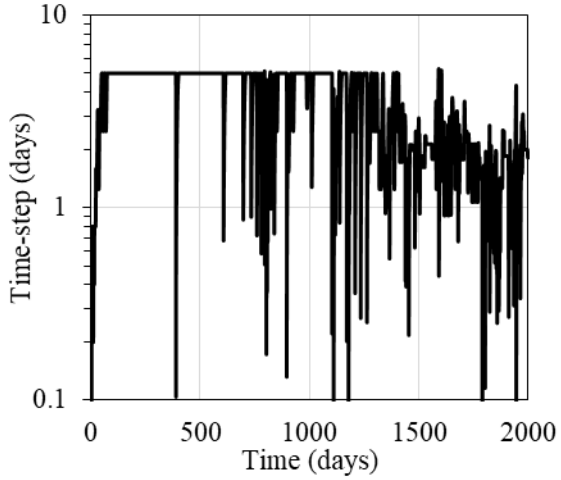


Figure 19. Time-step profile for Case 4.

# 6 CONCLUSIONS

In this work, the implementation of the natural variables fully implicit approach for a compositional reservoir simulation was presented. The new implementation considered advection, dispersion, up to four phases flow, and inactive cells, to mention some of the capabilities.

The new implementation was compared to the originally implemented IMPEC, which has been previously benchmarked with commercial simulators. The case studies presented considered heterogeneous properties and some cases considered irregular reservoir geometry. Such scenarios were really challenging for the IMPEC approach, which was not able to run any of the cases with inactive cells presented here, due to the complex phase behavior and large heterogeneity present in these cases. For the cases that IMPEC was able to run, the CPU time was excessive when compared to the natural variable implemented. Finally, the approach implemented was successful in running all cases.

# ACKNOWLEDGEMENTS

The authors would like acknowledge the sponsors of the RS-JIP of the Center for Petroleum and Geosystems Engineering at The University of Texas at Austin for the financial support. The authors also thank ScienceSoft for providing the S3Graf post-processor. The first and last authors would like to acknowledge CNPq (The National Council for Scientific and Technological Development of Brazil) for its financial support. We would also like to thanks Petrobras for financing support of this study.

# REFERENCES

Acs, G., Doleschall, S., & Farkas, E., 1985. General Purpose Compositional Model. *SPE Journal*. vol. 25, pp. 543–553.

Chang, Y., 1990. *Development and Application of an Equation of State Compositional Simulator*. PhD Dissertation, The University of Texas at Austin.

Chang, Y., Pope, G.A., & Sepehrnoori, K., 1990. A higher-order finite-difference compositional simulator. *Journal of Petroleum Science and Engineering*, vol. 5, pp. 35–50.

Chien, M.C.H., Lee, S.T., & Chen, W.H., 1985. A New Fully Implicit Compositional Simulator. In: *SPE Reservoir Simulation Symposium*.

Coats, K.H., 1980. An Equation of State Compositional Model. *SPE Journal*, vol. 20, pp. 363–376.

Collins, D.A., Nghiem, L.X., Li, Y.-K., & Grabonstotter, J.E., 1992. An Efficient Approach to Adaptive- Implicit Compositional Simulation with an Equation of State. *SPE Reservoir Engineering*, vol. 7, pp. 259–264.

dos Santos, L.O.S., Varavei, A., Sepehrnoori, K., 2013. A Comparison of Various Formulations for Compositional Reservoir Simulation. In: *SPE Reservoir Simulation Symposium*.

Fernandes, B.R.B., Marcondes, F., & Sepehrnoori, K., 2016. Comparison of Two Volume Balance Fully Implicit Approaches in Conjunction with Unstructured Grids for Compositional Reservoir Simulation. *Applied Mathematical Modelling*, vol. 40, pp. 5153–5170.

Fussell, L.T., & Fussell, D.D., 1979. An Iterative Technique for Compositional Reservoir Models. *SPE Journal*, vol. 19, pp. 211–220.

Khan, S.A., Pope, G.A., & Sepehrnoori, K., 1992. Fluid Characterization of Three-Phase CO2/Oil Mixtures. In: *SPE/DOE Enhanced Oil Recovery Symposium*.

Killough, J.E., & Kossack, C.A., 1987. Fifth Comparative Solution Project: Evaluation of Miscible Flood Simulators. In: *SPE Symposium on Reservoir Simulation*.

Maliska, C.R., 2004. *Computation Heat Transfer and Fluid Mechanics (In portuguese)*. Livros Tecnicos e Cientificos, Rio de Janeiro.

Michelsen, M.L., 1982. The isothermal flash problem. Part I. Stability. *Fluid Phase Equilibria*, vol. 9, pp. 1–19.

Nghiem, L.X., Fong, D.K., & Aziz, K., 1981. Compositional Modeling With an Equation of State. *SPE Journal*, vol. 21, pp. 687–698.

Peng, D.-Y., & Robinson, D.B., 1976. A New Two-Constant Equation of State. *Industrial Engineering Chemistry Fundamentals*, vol. 15, pp. 59–64.

Perschke, D.R., 1988. *Equation of State Phase Behavior Modelling for Compositional Simulator*. PhD Dissertation, The University of Texas at Austin.

Perschke, D.R., Chang, Y., Pope, G.A., & Sepehrnoori, K., 1989a. Comparison of Phase Behavior Algorithms for an Equation-Of-State Compositional Simulator. *SPE ELibrary*.

Perschke, D.R., Pope, G.A., & Sepehrnoori, K., 1989b. Phase Identification During Compositional Simulation. *SPE ELibrary*.

Trangenstein, J.A., 1987. Customized Minimization Techniques for Phase Equilibrium Computations in Reservoir Simulation. *Chemical Engineering Science*, vol. 42, pp. 2847–2863.

Wang, P., Yotov, I., Wheeler, M., Arbogast, T., Dawson, C., Parashar, M., & Sepehrnoori, K., 1997. A New Generation EOS Compositional Reservoir Simulator: Part I - Formulation and Discretization. In: *SPE Reservoir Simulation Symposium*.

Young, L.C., 1990. Use of Dispersion Relationships to Model Adverse-Mobility-Ratio Miscible Displacements. *SPE Reservoir Engineering*, vol. 5, pp. 309–316.

Young, L.C., & Stephenson, R.E., 1983. A Generalized Compositional Approach for Reservoir Simulation. *SPE Journal*, vol. 23, pp. 727–742.